

CONF-9704155--

Recent Electroweak Measurements from the Tevatron

Robert G. Wagner
For the CDF & DØ Collaborations

High Energy Physics Division
Argonne National Laboratory¹
Argonne, Illinois 60439-4815

RECEIVED
SEP 22 1997
OSTI

Abstract. Preliminary electroweak results are discussed from the Fermilab experiments, CDF and DØ, based on Tevatron run 1b data. These include an updated precision measurement of the W mass which when combined with previous Tevatron, CERN SppS, and LEP-II results gives a combined world average $M_W = 80.40 \pm 0.08 \text{ GeV}/c^2$. Also presented are new limits on anomalous gauge boson self-couplings, measurement of the W charge asymmetry, $\sigma \cdot B(W \rightarrow \tau \nu_\tau)$, and limits on quark-lepton compositeness from high mass Drell-Yan production.

I INTRODUCTION

The CDF and DØ collaborations have recently produced measurements of the W mass, M_W , based on integrated luminosities of 80 pb^{-1} (DØ) and 90 pb^{-1} (CDF) of data collected from run 1b of the Fermilab Tevatron collider. While precision measurement of M_W tests the Standard Model beyond the lowest order through radiative corrections to the mass, of more current interest is the simultaneous measurement of M_W and M_{top} and the constraint placed on the Higgs boson mass via loop corrections ($\Delta M_W \propto M_{top}^2, \ln M_{Higgs}$). In the next section I review the CDF and DØ W mass analysis and present both the preliminary run 1b results and the combined M_W estimate based on CDF, DØ, UA2, and LEP-II.

Additional electroweak physics results have been made available recently in preliminary form by DØ and CDF. In sections subsequent to the W mass review, I present results from DØ on gauge boson self-couplings from analysis of gauge boson pair production and on the $W \rightarrow \tau \nu_\tau$ branching ratio; and from CDF on the $W(\rightarrow e \nu_e, \mu \nu_\mu)$ charge asymmetry and on high mass

* Work supported in part by the U.S. Department of Energy,
Division of High Energy Physics, Contract W-31-109-ENG-38.

DISTRIBUTION OF THIS DOCUMENT IS UNLIMITED

MASTER
The submitted manuscript has been authored
by a contractor of the U. S. Government
under contract No. W-31-109-ENG-38.
Accordingly, the U. S. Government retains a
nonexclusive, royalty-free license to publish
or reproduce the published form of this
contribution, or allow others to do so, for
U. S. Government purposes.

DISCLAIMER

This report was prepared as an account of work sponsored by an agency of the United States Government. Neither the United States Government nor any agency thereof, nor any of their employees, makes any warranty, express or implied, or assumes any legal liability or responsibility for the accuracy, completeness, or usefulness of any information, apparatus, product, or process disclosed, or represents that its use would not infringe privately owned rights. Reference herein to any specific commercial product, process, or service by trade name, trademark, manufacturer, or otherwise does not necessarily constitute or imply its endorsement, recommendation, or favoring by the United States Government or any agency thereof. The views and opinions of authors expressed herein do not necessarily state or reflect those of the United States Government or any agency thereof.

DISCLAIMER

**Portions of this document may be illegible
in electronic image products. Images are
produced from the best available original
document.**

Drell-Yan lepton pair production with implications for limits on quark/lepton compositeness [1].

II CDF AND DØ M_W MEASUREMENTS

Precision measurement of the W mass is accomplished by analysis of $W \rightarrow e\nu_e$ or $\mu\nu_\mu$. In $\bar{p}p$ collisions, many of the particles are produced in the uninstrumented angular regions near the beam pipe which prevents measurement of the longitudinal momentum balance. With the preclusion of a direct reconstruction of the W mass, CDF and DØ rely on a model, first developed by the UA2 collaboration [2], that begins with measuring the components of momenta transverse to the beam axis and inferring the unobserved transverse energy of the decay neutrino, E_T^ν , from the E_T balance of the charged lepton, \vec{E}_T^ℓ , and the system recoiling from the W , \vec{u} :

$$\vec{E}_T^\nu = -(\vec{E}_T^\ell + \vec{u}). \quad (1)$$

The “transverse mass” of the W is then calculated from

$$(M_T^W)^2 = (E_T^\ell + E_T^\nu)^2 - (\vec{E}_T^\ell + \vec{E}_T^\nu)^2 = 2 | p_T^\ell || p_T^\nu | (1 - \cos \phi_{\ell\nu}). \quad (2)$$

Finally, M_W is extracted from a likelihood fit performed on the M_T^W lineshape by comparing data to Monte Carlo distributions generated for a range of M_W .

While CDF uses both the muon and electron decay modes for the precision measurement, the Tevatron run 1b electron channel mass analysis is still in progress and only results from the muon channel are presented here. DØ uses only the electron channel for the M_W measurement. Descriptions of the detectors are found in references [3,4]. For CDF, the muon momentum and direction are determined from reconstruction of the track in the Central Tracking Chamber (CTC) which is contained in a 1.4T solenoidal magnetic field. The DØ experiment determines the electron direction using the EM calorimeter cluster centroid and the associated track reconstructed in the tracking chamber and the energy is measured by calorimetry with the scale set by mass reconstruction of $\pi^0 \rightarrow \gamma\gamma$, $\psi \rightarrow e^+e^-$, and $Z \rightarrow e^+e^-$.

CDF selects ~ 21000 $W \rightarrow \mu\nu_\mu$ events having $25 \leq (p_T^\mu \& E_T) \leq 60$ GeV/c and recoil $| \vec{u} | \leq 20$ GeV. The muons must be minimum ionizing in the calorimetry and match with a stub segment in the muon drift chambers located radially outside the central calorimetry. Additional requirements are made to remove cosmic rays and Z events that were mis-identified due to having a muon in a region devoid of tracking. Finally, M_T^W is required to be in the range $50 - 120$ GeV/c². The M_T^W fit region of $65 - 100$ GeV/c² contains ~ 15000 events.

DØ obtains 28323 events for $W \rightarrow e\nu_e$ requiring $(p_T^e \& E_T) > 25$ GeV and $| \vec{u} | < 15$ GeV/c. Electrons are required to have an EM calorimeter cluster

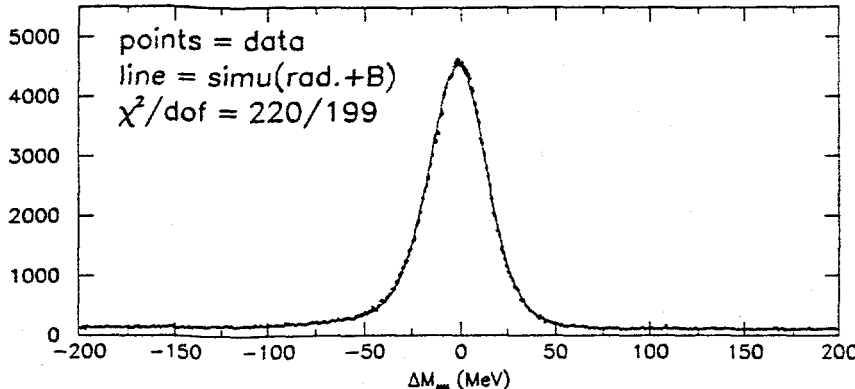


FIGURE 1. The mass difference between $J/\psi \rightarrow \mu^+\mu^-$ observed in the CDF tracking chamber and the world average M_ψ . Data are represented by points and the solid curve is the best fit to a simulated lineshape including contributions from radiative decay of the J/ψ and non-prompt J/ψ production in B -meson decays.

that matches with a track in the central detector, an electron-like shower shape, and the energy in an annular ring of $\Delta R \equiv \sqrt{(\Delta\eta)^2 + (\Delta\phi)^2} = 0.2 - 0.4$ centered on the electron must be less than 15% of the electron energy.

Both experiments also select Z event samples for energy/momentum scale calibration and checking.

The CDF M_W measurement begins with a determination of the CTC momentum scale by fitting the $J/\psi \rightarrow \mu^+\mu^-$ mass spectrum obtained from a sample of $\sim 250,000$ events and comparing to the world average value. The reconstructed muon momentum is corrected for energy lost during traversal of the detector; run-to-run magnetic field variation; and geometric misalignment of the magnet, beam, and CTC. Figure 1 shows the difference between the reconstructed J/ψ mass and the world average value. The measured M_ψ is 3096.2 ± 1.5 MeV/c² with the dominant contributions to the uncertainty attributed to knowledge of muon energy loss in the detector (1.0 MeV) and possible variation of the momentum scale with increasing muon transverse momentum (1.0 MeV). Comparison to the Particle Data tables M_ψ [5] gives a momentum scale correction factor, 1.00023 ± 0.00048 . The uncertainty of ± 1.5 MeV/c² extrapolated from M_ψ to M_W implies a contribution from momentum scale of $\delta M_W = \pm 40$ MeV/c².

DØ parametrizes the energy measured in the EM calorimeter as

$$E_{\text{meas}} = \alpha_{\text{EM}} E_{\text{true}} + \delta_{\text{EM}} \quad (3)$$

$$\alpha_{\text{EM}} \equiv \text{energy scale factor}, \quad \delta_{\text{EM}} \equiv \text{offset}$$

Measured values of $\pi^0 \rightarrow \gamma\gamma$ and $J/\psi, Z^0 \rightarrow e^+e^-$ masses are linear in the coefficients, α_{EM} and δ_{EM} , and provide intersecting elliptical constraints on

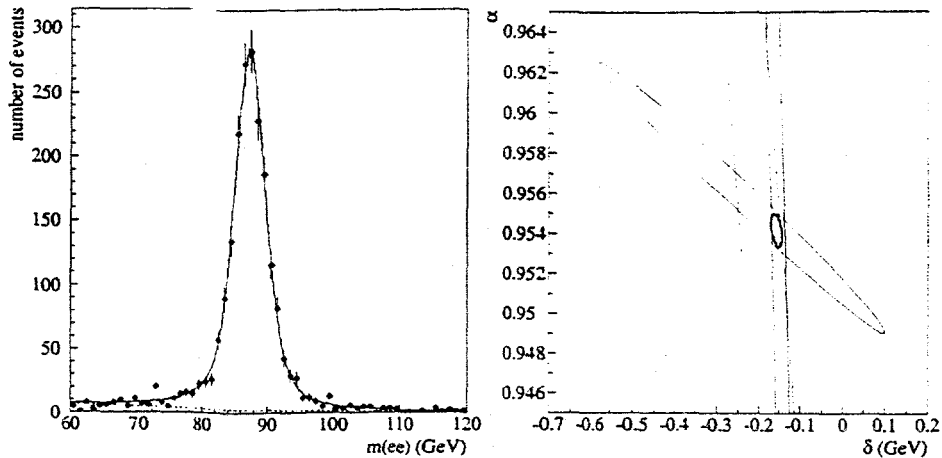


FIGURE 2. Fitted DØ Z mass used for energy scale calibration (left). The π^0 and J/ψ mass plots are not shown. Elliptical constraints on EM scale calibration parameters, α_{EM} and δ_{EM} based on measurements of π^0 , J/ψ , and Z^0 masses (right).

them (see figure 2). The values for the parameters extracted using the data of figure 2 are $\alpha_{\text{EM}} = 0.95372 \pm 0.00091$ and $\delta_{\text{EM}} = -0.16^{+0.03}_{-0.21}$ GeV.

The components of the recoil model are the W transverse momentum, p_T^W , and the hadronic recoil response of the calorimetry. Both experiments use the next-to-leading order calculation of p_T^W due to Arnold and Kauffman [6] supplemented by a low p_T^W parametrization of Ladinsky and Yuan [7].

CDF derives the response function using the recoil hadron-dielectron momentum balance for a sample of Z events and the resolution function is determined from minimum bias trigger data. The adequacy of the model is checked using the recoil observed in Z data and the u_\perp distribution from the W data. The u_\perp axis is defined as that perpendicular to the W decay muon.

Similarly, DØ extracts both the response and resolution functions from $Z \rightarrow e^+e^-$ data. Recoil components along the angular bisector of the e^+e^- pair are added as are those normal to the bisector. The response and resolution are tuned via Monte Carlo simulation to reproduce the observed distributions.

W events for a range of M_W are generated and processed through detector simulations. Likelihood values are calculated comparing to the observed M_T^W distribution and M_W is extracted from a fit to the log-likelihood function. The M_T^W distributions with the best fits overlaid are shown in figure 3. Table 1 gives the systematic uncertainty contributions for both measurements. The preliminary Tevatron run 1b values are $M_W(\text{CDF}) = 80.430 \pm 0.100 \text{ (stat)} \pm 0.155 \text{ (syst)} \text{ GeV}/c^2$ and $M_W(\text{DØ}) = 80.45 \pm 0.10 \text{ (stat)} \pm 0.07 \text{ (syst)} \text{ GeV}/c^2$. The DØ statistical uncertainty is a combination of $\pm 70 \text{ MeV}/c^2$ from the fit and $\pm 65 \text{ MeV}/c^2$ from normalization to the world average Z mass. CDF expects to improve the systematic uncertainty somewhat as the recoil model analysis is improved. A

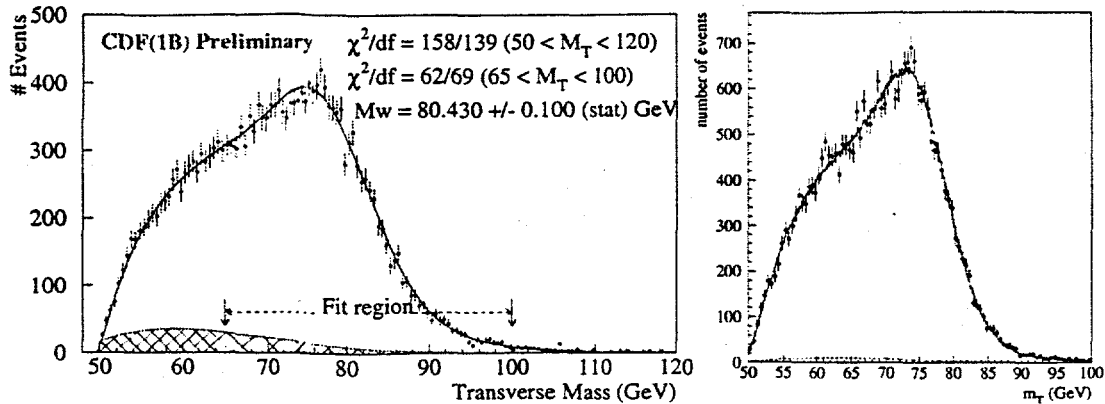


FIGURE 3. The CDF(left) and DØ(right) W transverse mass distributions (points) with best fits from Monte Carlo overlaid (solid line). Cross-hatched (CDF) and dotted (DØ) curves indicate the combined background from $W \rightarrow \tau\nu_\tau$, mis-identified Zs, QCD di-jets, and, for the CDF muon channel, residual cosmic ray events.

summary of precision W mass measurements is given in figure 4 along with the corresponding constraint on M_{Higgs} provided by M_W vs M_{top} .

III GAUGE BOSON SELF-COUPLEDINGS

Electroweak theory specifies all fermion and gauge boson couplings. While the coupling of leptons and quarks to gauge bosons has been well-measured, the gauge bosons' couplings to themselves is not yet verified to be that of the Standard Model. At the Tevatron all combinations of pair production of W^\pm, Z^0 , and γ are kinematically accessible allowing measurement of standard tri-linear couplings such as WWZ and $WW\gamma$ as well as searches for non-standard couplings such as $ZZ\gamma$.

DØ has completed analysis of $W\gamma$ production for all of Tevatron run 1a + run 1b. Event selection requires a high E_T charged lepton (μ or e), $E_T > 25$ GeV, and a photon with $E_T \geq 10$ GeV. The radiative W decay contribution is reduced relative to direct production from the W propagator by requiring the lepton-photon angular separation to be greater than 0.7. The main background is from $W+jets$ in which the fragmentation of one of the jets fakes a photon signature. The background-subtracted number of $W\gamma$ events is $84^{+12}_{-11}(\text{stat}) \pm 9(\text{syst})$, giving a cross section

$$\sigma(\bar{p}p \rightarrow W\gamma \rightarrow \ell\nu\gamma) = 11.3^{+1.7}_{-1.5}(\text{stat}) \pm 1.5(\text{sys}) \text{ pb}$$

$$\text{Std. Model : } \sigma(\bar{p}p \rightarrow W\gamma \rightarrow \ell\nu\gamma) = 12.5 \pm 1.0 \text{ pb}$$

Figure 5 shows the photon E_T , $\ell - \gamma$ angular separation, and $W\gamma$ minimum invariant (also called transverse cluster) mass. A binned likelihood fit to the

TABLE 1. Statistical and systematic uncertainty contributions for the preliminary run 1b CDF and DØ W mass measurements

Preliminary Uncertainty	ΔM_W^μ MeV/c ² CDF 1b	ΔM_W^ϵ MeV/c ² DØ 1b
I. Statistical	100	70 ± 65
II. Momentum Scale	40	—
Calorimeter linearity	—	20
Electron polar angle	—	28
III. Other Systematics	115	60
1. Resolution	25	23
2. Input p_T^W	40	5
3. Recoil modeling	90	39
4. Parton dist. fcn.	25	21
5. Selection bias	10	—
6. Trigger bias	15	—
7. Radiative corr.	20	20
8. Higher-order corr.	20	—
9. Backgrounds	25	12
10. Fitting	10	—
11. W width	—	9
12. Calorimeter uniformity	—	10
13. Parton luminosity	—	10
14. Lepton removal	—	16
Total systematics	122	70
TOTAL UNCERTAINTY	155	118

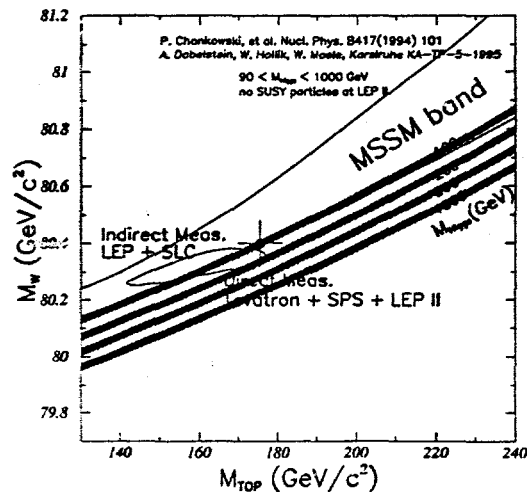
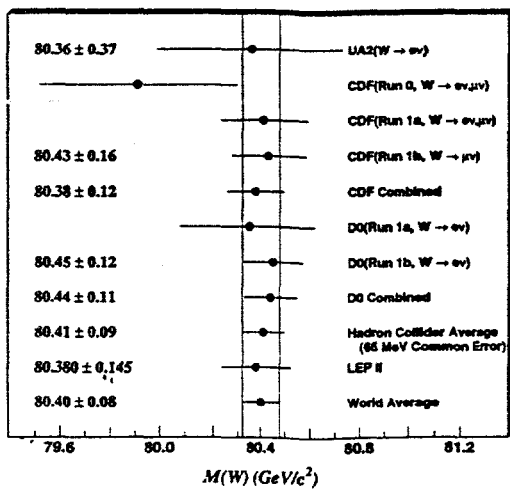


FIGURE 4. Summary of existing precision M_W measurements (left). The righthand plot shows the combined measurement for M_W vs. M_{top} with M_{Higgs} bands from loop corrections overlaid.

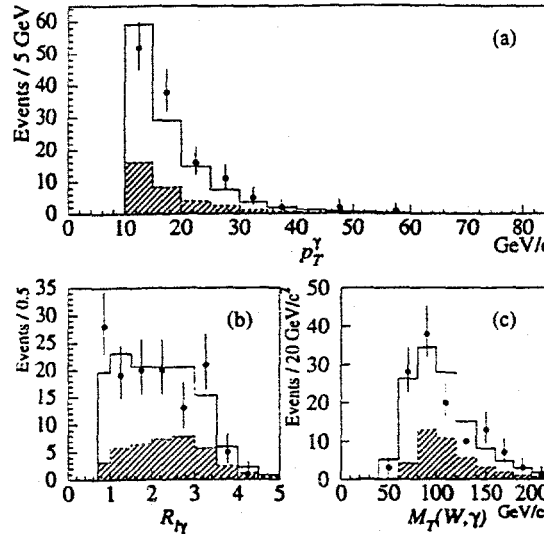


FIGURE 5. From the DØ $W\gamma$ analysis are shown the (a) photon p_T spectrum, (b) charged lepton-photon angular separation, and (c) $W\gamma$ minimum invariant mass. Shaded regions indicate estimated background and the open histogram is the background plus Standard Model expectation.

photon E_T spectrum is used to provide 2-d contour limits on anomalous $WW\gamma$ couplings, $\Delta\kappa_\gamma$ and λ [8]. One dimensional limits are derived by setting one of the couplings to zero and extracting the 95% c.l. for the other from the likelihood function. Thus,

$$\left. \begin{array}{l} -0.93 < \Delta\kappa_\gamma < 0.94 \\ -0.31 < \lambda < 0.29 \end{array} \right\} \begin{array}{l} (\text{for } \lambda = 0) \\ (\text{for } \Delta\kappa_\gamma = 0) \end{array} \} 95\% \text{ c.l.}$$

DØ and CDF have searched for $Z\gamma$ coupling, a phenomenon not present in Electroweak theory. Run 1a results have been published and CDF has previously presented preliminary results from run 1b based on a 67 pb^{-1} partial sample. From all run 1b data, DØ has produced in preliminary form a search for $\bar{p}p \rightarrow Z(\rightarrow e^+e^-) + \gamma + X$ selecting events in a similar manner to those of $W\gamma$ except there is no E_T requirement and $M(e^+e^-)$ must be consistent with M_Z . For the CP-conserving couplings, h_{30}^Z and h_{40}^Z [9], 2-d limits are shown in figure 6. The unitarity limit is particularly sensitive to the form factor scale used and has been set to $\Lambda_{\text{FF}} = 500 \text{ GeV}$ for all limits shown in the figure with the exception of that for L3. The most stringent limit derives from the DØ run 1a analysis of the mode $Z(\rightarrow \nu\bar{\nu}) + \gamma$ which has the advantage of having no competing radiative decay mode and is sensitive to all neutral decays of the Z^0 . The photon E_T requirement was raised to $E_T^\gamma > 40 \text{ GeV}$ to remove background from $W \rightarrow e\nu_e$ events where the electron is mis-identified as a photon due to lack of an associated track. Since anomalous couplings mainly

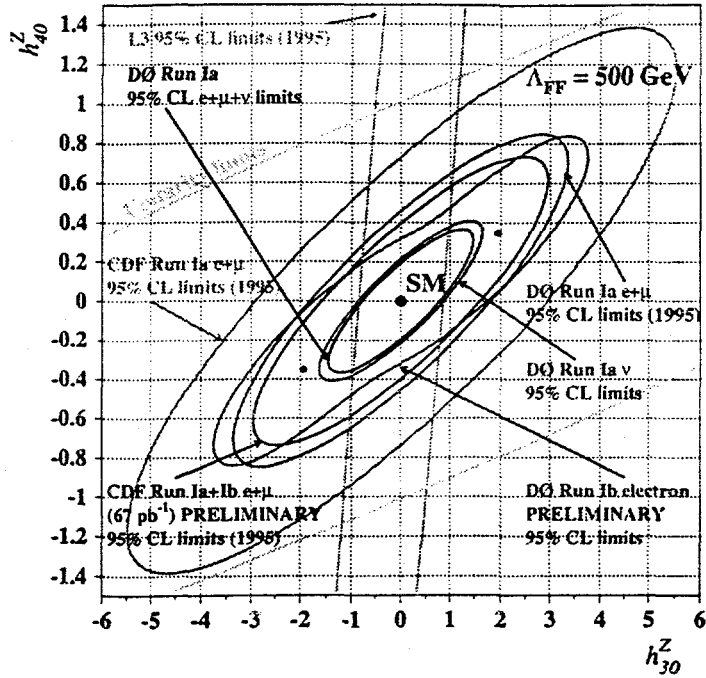


FIGURE 6. Two dimensional contour limits for anomalous CP-conserving couplings for $ZZ\gamma$. See text for explanation of form factor scale and other details.

enhance the high E_T^γ region, this has little effect on the coupling limit. From analyses of WW and WZ production, limits on $\Delta\kappa_{Z,\gamma}$ and $\lambda_{Z,\gamma}$ have been obtained for both DØ (preliminary run 1b) and CDF (final run 1b). These are not covered here due to space limitations. The public Electroweak Web pages [1] for both groups contain full details of the analyses which provide limits comparable to those presented above for $W\gamma$.

IV CDF W CHARGE ASYMMETRY

Due to parity violation in the weak interaction a forward/backward asymmetry occurs in $W \rightarrow \ell\nu_\ell$. CDF has measured the asymmetry between W^+ and W^- as a function of the charged lepton pseudorapidity using both the electron and muon decay channels. Because the proton u -quark parton distribution function, $u(x)$, is greater than that of the d -quark, $d(x)$, the $W^+(W^-)$ is boosted along the $p(\bar{p})$ direction and the observed asymmetry is most sensitive to the choice of PDF. This PDF constraint has proved useful in reducing the systematic uncertainty contribution to the W mass.

Although 3-d track reconstruction using the CTC is unavailable beyond $|\eta| \sim 1.2$, the measurement has been extended to $|\eta| \simeq 2.0$ by using the expected correspondence between a track in the CDF silicon microtracker and

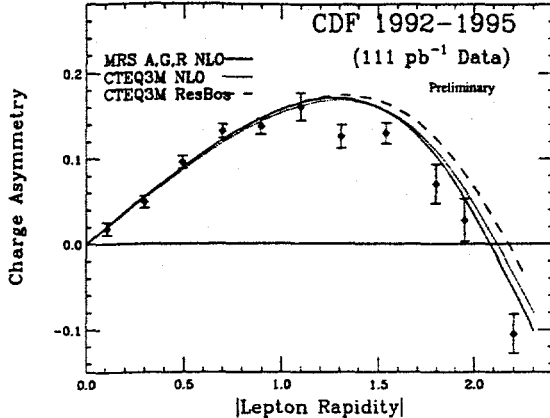


FIGURE 7. The charged lepton asymmetry, as measured by CDF, between W^+ and W^- as a function of charged lepton pseudorapidity.

the plug EM calorimeter. A point at $|\eta| = 2.2$ is provided via the CDF forward muon detector. Results are shown in figure 7 along with expectations due to various choices of PDF.

V DØ $\sigma \cdot B(W \rightarrow \tau \nu_\tau)$

DØ has improved the previous CDF measurement [10] of the cross section times branching ratio for $W \rightarrow \tau \nu_\tau$ using the hadronic decay of the τ which is identified as an isolated narrow jet. Events selected had $E_T(jet) > 25$ GeV ($|\eta| < 0.9$) and $E_T > 25$ GeV. Signal and background were estimated from the distribution of a variable designated, Profile \equiv (sum of highest two tower E_T)/(cluster E_T). Profile < 0.35 was designated the background region and Profile > 0.55 constituted the signal region. The background in the τ signal region was estimated using a QCD sample. Table 2 details the event number breakdown. The cross section is $\sigma \cdot B(W \rightarrow \tau \nu_\tau) = 2.38 \pm 0.09 \pm 0.10$ nb, where the luminosity uncertainties have not been included. This gives a coupling relative to that for the electron of $g_\tau^W/g_e^W = 1.00 \pm 0.02 \pm 0.03$; consistent with lepton universality.

VI DRELL-YAN COMPOSITENESS LIMITS

CDF has searched in Drell-Yan production at the Tevatron for evidence of quark or lepton compositeness. Substructure would add a contact term to the dilepton production amplitude and manifest itself mainly in the interference with the Standard Model amplitude. Interaction strengths for the contact term are assumed to be of the form, $\xi_{ij} = \pm g_o^2/\Lambda_{ij}^2$, where i, j are the helicities. The compositeness scale, Λ_{ij} , is defined assuming $g_o^2/4\pi = 1$. The

TABLE 2. DØ $W \rightarrow \tau \nu_\tau$ Results

Event Source	Number of Events
Final Data Sample	1202
QCD Background	$106 \pm 7 \pm 5$
Noise Events	81 ± 14
$Z \rightarrow \tau^+ \tau^-$	32 ± 5
$W \rightarrow e \nu_e$	3 ± 1

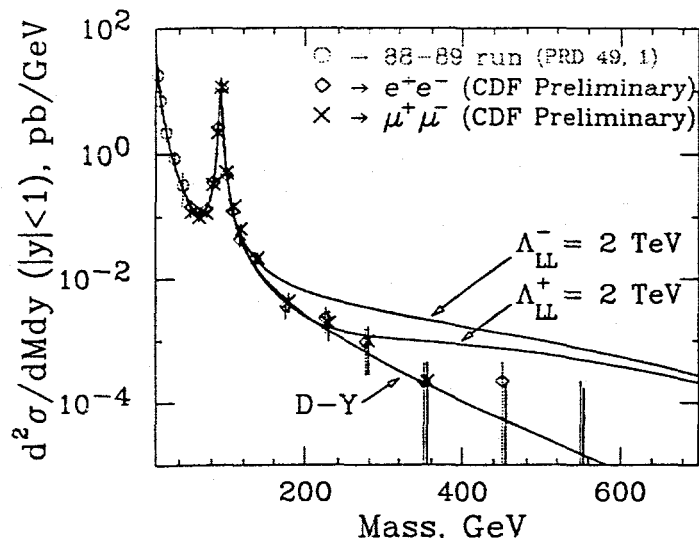


FIGURE 8. The differential mass cross section for a tightly selected isolated lepton plus a second lepton with looser selection criteria. QCD background was estimated from same sign lepton pairs while $WW, \tau\tau, c\bar{c}$, etc. backgrounds were estimated from $e\mu$ pairs.

dilepton differential mass spectrum for rapidity less than 1 is plotted and normalized to the region around M_Z , specifically $50 < M(\ell^+ \ell^-) < 150$ GeV/c². A binned likelihood is calculated for the region $M(\ell^+ \ell^-) > 150$ GeV/c² and 95% confidence level limits are determined for a contact term for a variety of helicity assumptions. Figure 8 shows the mass spectrum along with expectations for a totally left-handed contact term at a compositeness scale of 2 TeV. Assuming quark and lepton universality in compositeness, limits on Λ^+ (positive sign of coupling) range from $> 3.0 - 5.0$ TeV, while for Λ^- the range is $> 3.7 - 6.3$ TeV for a compositeness scale.

VII SUMMARY

The Tevatron run 1b integrated luminosity increase of 5-6 over run 1a halved the uncertainty of M_W . DØ has significantly tightened limits on anomalous

gauge boson couplings; especially from analysis of the $Z \rightarrow \nu\bar{\nu}$ decay channel. Run 1b has also witnessed the first observation of WW , WZ , and ZZ production. Pseudorapidity region coverage for the W charge asymmetry has doubled to $|\eta| \sim 2.2$ providing improved constraints on parton distribution functions. DØ has demonstrated lepton universality through the measurement of $\sigma \cdot B(W \rightarrow \tau\nu_\tau)$. Analysis of Drell-Yan production has allowed CDF to push the compositeness scale limits to greater than 3-6 TeV depending on the helicity and sign of the coupling assumed.

In run 2, DØ and CDF will continue precision electroweak sector measurements. The W mass uncertainty should be reduced to near ± 40 MeV/c². Limits on anomalous gauge boson self-couplings will continue to improve and observation of the radiation amplitude zero in $W\gamma$ production [11] will be addressed.

I thank the organizers of the Beyond the Standard Model V conference for a well run, informative, and enjoyable conference in a beautiful location. I am indebted to the members of the DØ and CDF electroweak physics groups for help in obtaining the latest results and plots, and for comments on the manuscript.

REFERENCES

1. The most current electroweak results are available on the public World Wide Web page each experiment maintains:
CDF — www-cdf.fnal.gov/physics/ewk/ewk.html
DØ — www-d0.fnal.gov/public/wz/ewk_public.html
2. Alitti, J. *et al.*, *Phys. Lett. B* **241**, 150 (1990).
3. Abe, F. *et al.*, *Nucl. Instrum. Methods A* **271**, 387 (1988); Abe, F. *et al.* *Phys. Rev. D* **50**, 2966 (1994); Amidei, D. *et al.* *Nucl. Instrum. Methods A* **350**, 73 (1994).
4. Abachi, S. *et al.*, *Nucl. Instrum. Methods A* **338**, 185 (1994).
5. Particle Data Group: Barnett, R. M. *et al.*, *Phys. Rev. D* **54** Part I, 530 (1996).
6. Arnold, P. B. and R. P. Kauffman, *Nucl. Phys. B* **349**, 381 (1991).
7. Ladinsky, G. A. and C.-P. Yuan, *Phys. Rev. D* **50**, 4239 (1994).
8. Hagiwara, K. *et al.*, *Nucl. Phys. B* **282**, 253 (1987).
9. Baur, U. and E. L. Berger, *Phys. Rev. D* **47**, 4889 (1993).
10. Abe, F. *et al.*, *Phys. Rev. Lett.* **68**, 3398 (1992).
11. Brown, R. W., K. Kowalski, and S. J. Brodsky, *Phys. Rev. D* **28**, 624 (1983).